Separation and Purification Technology 282 (2022) 120110

Contents lists available at ScienceDirect

Separation and Purification Technology

journal homepage: www.elsevier.com/locate/seppur

Modelling of lithium extraction with TBP/P507–$FeCl_3$ system from salt-lake brine

Hui Su [a,b,1], Boren Tan [a,b,c,1], Jian Zhang [a,b,c], Wensen Liu [d], Lina Wang [a,b], Yong Wang [a,b,*], Zhaowu Zhu [a,b,e,*], Tao Qi [a,b]

[a] National Engineering Research Center of Green Recycling for Strategic Metal Resources, Beijing 100190, China
[b] Key Laboratory of Green Process and Engineering, Institute of Process Engineering, Chinese Academy of Sciences, Beijing 100190, China
[c] School of Chemistry and Chemical Engineering, University of Chinese Academy of Sciences, Beijing 101408, China
[d] School of Chemical and Environmental Engineering, China University of Mining and Technology (Beijing), Beijing 100083, China
[e] Innovation Academy for Green Manufacture, Chinese Academy of Sciences, Beijing 100190, China

ARTICLE INFO

Keywords:
Lithium
Solvent extraction
Salt-lake brine
TBP/P507
Modelling

ABSTRACT

Recovery of lithium from Mg-rich salt-lake brines by solvent extraction has been widely studied for high Li^+/Mg^{2+} selectivity and Li^+ extraction efficiency. In a previous study, a ternary synergistic solvent extraction system consisting of tributyl phosphate (TBP), 2-ethylhexyl phosphonic acid mono-2-ethylhexyl ester (P507, denoted as HL) and $FeCl_3$ was developed, in which high Li^+ selectivity and efficient Li^+ stripping simply with water were realized. In this study, to further elucidate the extraction mechanism of the TBP/P507/$FeCl_3$ system and minimize the efforts on the process optimization for Li extraction from Mg-rich salt-lake brines with different component concentrations from different sources, a thermodynamic empirical model based on mass balances and equilibrium equations has been developed. The model parameters were optimized by fitting the calculated data to experimental results. By calculating the distribution of species in the organic phase with the model, it was found that Li^+ primarily existed in the form of $[Li(TBP)_2][FeCl_4]$, followed by $[Li(TBP)][FeCl_4]$. When Li^+ was stripped with water, Fe^{3+} mainly existed in the form of $FeCl_2L{\cdot}HL{\cdot}2TBP$ in the organic phase at low O/A ratios but converted to $[H(TBP)_2][FeCl_4]$ at high O/A ratios. This thermodynamic model provides a guide for the design of practical process flow.

1. Introduction

New-energy electric vehicles driven by lithium-ion battery (LIB) have been advanced rapidly in recent years. They replace the conventional fossil-fuel-powered vehicles and achieve zero CO_2 emission, which is in line with the goal of “carbon neutralization” [1]. Driven by the increasing popularity of electric vehicles, not only has the share of lithium (Li) used in batteries increased to 65% of the global Li consumption in 2019 [2], the global Li demand is also expected to continuously grow in the future. In 2019, the global demand for lithium carbonate equivalent (LCE) is about 300,000 tons. By 2025, it will exceed 870,000 tons [2,3].

Hard rock and salt-lake brine are the two main primary sources of Li, accounting for 34% and 61% of the total reserve, respectively [4]. Currently, more than half of Li_2CO_3 (or equivalent) is produced from salt-lake brine [5,6]. The Li resources of salt-lake brine in China account for >80% [7], which are mainly distributed in Qinghai and Tibet. Among them, salt-lake Li in Qinghai accounts for about 54%, and lithium chloride (LiCl) reserves reach 19.82 million tons [7,8]. However, these salt-lake brines have high magnesium (Mg) contents and very high Mg/Li ratios (>50) [9], resulting in a large challenge for Li recovery since Li and Mg have very similar physicochemical properties.

In recent years, progress has been made in several separation techniques for the recovery of Li from Mg-rich brines, including solvent extraction [10-15], membrane separation [16-18], adsorption [19-21], and electrochemical methods [22,23]. Among them, the solvent extraction method based on a TBP/$FeCl_3$ system is particularly suitable for Li recovery from brine with high Mg/Li ratios because of the high Li/Mg selectivity and low capital and operational costs [13,24-27]. However, the system uses high concentration HCl (6–8 mol L^{-1}) to strip Li by

---

[*] Corresponding authors at: National Engineering Research Center of Green Recycling for Strategic Metal Resources, Beijing 100190, China.
E-mail addresses: wangyong@ipe.ac.cn (Y. Wang), zhwzhu@ipe.ac.cn (Z. Zhu).

[1] These authors contributed equally to this work and should be considered co-first authors.

https://doi.org/10.1016/j.seppur.2021.120110
Received 11 October 2021; Received in revised form 2 November 2021; Accepted 4 November 2021

replacing Li^{+} with H^{+}, which is easy to cause TBP degradation and equipment corrosion. Meanwhile, the organic phase needs to consume a large amount of alkaline reagent to neutralize the extracted excess acid, so as to realize its regeneration and recycling. And the refining process of Li products is complicated, resulting in the high cost of Li recovery.

Recently, it has been found that some ionic liquids (ILs) containing $[PF_6]^{-}$ [28], $[BPh_4]^{-}$ [29], $[NTf_2]^{-}$ [30], or $[PW_{12}O_{40}]^{3-}$ [31] anions can form a composite system with TBP for synergistic extraction of Li^{+}. These ILs eliminate the use of $FeCl_3$ and improve the extraction efficiency of Li^{+}. However, ILs containing these anions are expensive and suffer from recycling difficulties, and they still cannot actually improve Li^{+} stripping, and hence, they are not suitable for industry scale production.

A ternary synergistic solvent extraction system TBP/P507/$FeCl_3$ was developed in our previous study [32,33], in which Li^{+} was stripped with water instead of high concentration HCl through the regulation of Fe^{3+} coordination. Li^{+} was extracted into the organic phase by forming the $[Li(TBP)_2][FeCl_4]$ complex, while P507 was not involved in the coordination. When Li^{+} was stripped by water, P507 and TBP synergistically coordinated with Fe^{3+} in the form of $[FeCl_2L\cdot(HL)\cdot 2TBP]$ (HL denotes P507), leading to efficient stripping of Li due to the broken structure of $[Li(TBP)_2][FeCl_4]$. The organic phase loaded with Fe^{3+} can be recycled directly without regeneration, and the cost of recovering Li from salt-lake brines is significantly reduced.

However, there are still some issues about the extraction and stripping mechanism of the TBP/P507/$FeCl_3$ system to be elucidated due to the complexity of the extracted species of Li^{+}, Mg^{2+}, H^{+} and Fe^{3+} in the organic phase under the relevant operating conditions. Meanwhile, little research has been focused on the optimization of the separation processes for Li extraction when TBP/P507/$FeCl_3$ system was applied to Mg-rich salt-lake brines with different component concentrations from different sources. Determining such conditions experimentally is laborious and time-consuming. For these reasons, this study aims to develop a thermodynamic empirical model based on mass balances and equilibrium equations in order to further clarify the extraction mechanism of the system and minimize the efforts on the optimization process. The model parameters were optimized by fitting the calculated data to the experimental results. The concentration of each species in the loaded organic phase after extraction was derived from the model as a function of the concentration of TBP and HCl, respectively. The residual concentration of each species in the organic phase after stripping was also derived from the model as a function of phase ratio (O/A).

2. Modelling

2.1. *Chemical reaction equilibrium in TBP/P507/$FeCl_3$ system*

The chemical reaction equilibrium and corresponding expression of apparent equilibrium constant involved in extracting Li^{+} from Mg-rich salt-lake brine by TBP/P507/$FeCl_3$ system are shown in Table 1. The overbar indicates that the compound resides in the organic phase. In the extraction process, Li^{+} is mainly extracted by TBP and combined with $FeCl_4^{-}$ to balance the charge, in which the number of TBP molecules participating in the reaction is 1 or 2 (Eqs. (13) and (14)) [24,34,35]. Competitive extraction occurs between H^{+} and Li^{+}, and the extraction equilibrium of H^{+} is shown in Eq. (12). Meanwhile, H^{+} can be extracted by TBP in the form of $HCl\cdot TBP$ (Eq. (11)) [36-39].

Table 1

Equilibrium and corresponding expression of equilibrium constant in TBP/P507/$FeCl_3$ system implemented in the model.

No.	Equilibrium	Equilibrium constant
(1)	$Fe^{3+} + Cl^{-} \rightleftharpoons FeCl^{2+}$	$k_1 = \frac{[FeCl^{2+}]}{[Fe^{3+}][Cl^{-}]}$
(2)	$Fe^{3+} + 2Cl^{-} \rightleftharpoons FeCl_2^{+}$	$k_2 = \frac{[FeCl_2^{+}]}{[Fe^{3+}][Cl^{-}]^2}$
(3)	$Fe^{3+} + 3Cl^{-} \rightleftharpoons FeCl_3$	$k_3 = \frac{[FeCl_3]}{[Fe^{3+}][Cl^{-}]^3}$
(4)	$Fe^{3+} + 4Cl^{-} \rightleftharpoons FeCl_4^{-}$	$k_4 = \frac{[FeCl_4^{-}]}{[Fe^{3+}][Cl^{-}]^4}$
(5)	$\overline{HL} \rightleftharpoons HL$	$k_{HL,1} = \frac{[HL]}{[\overline{HL}]}$
(6)	$2\overline{HL} \rightleftharpoons \overline{(HL)_2}$	$k_{HL,2} = \frac{[(\overline{HL})_2]}{[\overline{HL}]^2}$
(7)	$HL \rightleftharpoons L^{-} + H^{+}$	$k_{HL,3} = \frac{[L^{-}][H^{+}]}{[HL]}$
(8)	$\overline{TBP} \rightleftharpoons TBP$	$k_{T,1} = \frac{[TBP]}{[\overline{TBP}]}$
(9)	$\overline{(HL)_2} + \overline{TBP} \rightleftharpoons \overline{(HL)_2 - TBP}$	$k_{T,2} = \frac{[\overline{(HL)_2 - TBP}]}{[\overline{TBP}][\overline{(HL)_2}]}$
(10)	$\overline{(HL)_2} + 2\overline{TBP} \rightleftharpoons \overline{(HL)_2 - (TBP)_2}$	$k_{T,3} = \frac{[\overline{(HL)_2 - (TBP)_2}]}{[\overline{TBP}]^2[\overline{(HL)_2}]}$
(11)	$H^{+} + Cl^{-} + \overline{TBP} \rightleftharpoons \overline{HCl\cdot TBP}$	$k_{T,4} = \frac{[\overline{HCl\cdot TBP}]}{[\overline{TBP}][H^{+}][Cl^{-}]}$
(12)	$H^{+} + FeCl_4^{-} + 2\overline{TBP} \rightleftharpoons \overline{[H(TBP)_2][FeCl_4]}$	$k_5 = \frac{[\overline{[H(TBP)_2][FeCl_4]}]}{[\overline{TBP}]^2[FeCl_4^{-}][H^{+}]}$
(13)	$Li^{+} + FeCl_4^{-} + \overline{TBP} \rightleftharpoons \overline{[Li(TBP)][FeCl_4]}$	$k_{L,1} = \frac{[\overline{[Li(TBP)][FeCl_4]}]}{[\overline{TBP}][FeCl_4^{-}][Li^{+}]}$
(14)	$Li^{+} + FeCl_4^{-} + 2\overline{TBP} \rightleftharpoons \overline{[Li(TBP)_2][FeCl_4]}$	$k_{L,2} = \frac{[\overline{[Li(TBP)_2][FeCl_4]}]}{[\overline{TBP}]^2[FeCl_4^{-}][Li^{+}]}$
(15)	$Mg^{2+} + 2FeCl_4^{-} + x\overline{TBP} \rightleftharpoons \overline{[Mg(TBP)_x][FeCl_4]_2}$	$k_{M,1} = \frac{[\overline{[Mg(TBP)_x][FeCl_4]_2}]}{[\overline{TBP}]^x[FeCl_4^{-}]^2[Mg^{2+}]}$
(16)	$Mg^{2+} + 2Cl^{-} + y\overline{HL} + z\overline{TBP} \rightleftharpoons \overline{[MgCl_2]HL_y\cdot TBP_z}$	$k_{M,2} = \frac{[[\overline{MgCl_2}]HL_y\cdot TBP_z]}{[\overline{HL}]^y[\overline{TBP}]^z[Mg^{2+}][Cl^{-}]^2}$
(17)	$FeCl_2^{+} + \overline{(HL)_2} + 2\overline{TBP} \rightleftharpoons \overline{FeCl_2L\cdot(HL)\cdot 2TBP} + H^{+}$	$k_{Fe} = \frac{[\overline{FeCl_2L\cdot(HL)\cdot 2TBP}][H^{+}]}{[\overline{TBP}]^2[FeCl_2^{+}][\overline{(HL)_2}]}$

In the presence of Fe^{3+}, the extracted species of Mg^{2+} are complicated. It has been proposed that Mg^{2+} is extracted in the form of $[Mg(TBP)_2][FeCl_4]_2$[24,40], but no targeted research has been carried out to prove this assumed composition. As a consequence, the extraction form of Mg^{2+} in this model was expressed as $[Mg(TBP)_x][FeCl_4]_2$, where × is the number of TBP molecules involved in the reaction. The value of × can be further determined through model calculation. If this assumption is reasonable, the concentration of Mg^{2+} and Fe^{3+} in the organic phase should meet the ratio of $[Mg^{2+}]/[Fe^{3+}] = 1:2$. Moreover, since the coordination ratio of Fe^{3+} to Li^{+} and H^{+} in the organic phase is 1:1 in both cases, it is known that the concentrations of Mg^{2+}, Fe^{3+} and Li^{+} in the organic phase need to meet the relationship of $2[Mg^{2+}] < ([Fe^{3+}]-[Li^{+}])$. However, it can be seen from Table 2 that the relationship they actually follow is $2[Mg^{2+}] \gg ([Fe^{3+}]-[Li^{+}])$[33]. This indicates that Mg^{2+} extracted into the organic phase should exist in different forms apart from $[Mg(TBP)_x][FeCl_4]_2$. In our previous study [33], the organic phase loaded with Li and Mg was scrubbed with water at an O/A ratio of 40:1, the scrubbing of Mg^{2+} was as high as 74.4%, indicating that part of Mg^{2+}

Table 2
Fe^{3+} and Mg^{2+} concentrations in organic phase at various TBP concentrations [33]

[TBP] (%)	$[Fe^{3+}]_{org}$ (mol/L)	$[Mg^{2+}]_{org}$ (mol/L)	$[Li^{+}]_{org}$ (mol/L)	$[Fe^{3+}]_{org}$-$[Li^{+}]_{org}$(mol/L)	$2[Mg^{2+}]_{org}$(mol/L)
40	0.24	0.09	0.16	0.08	0.18
45	0.24	0.12	0.16	0.08	0.25
50	0.24	0.15	0.15	0.09	0.30
55	0.24	0.21	0.17	0.07	0.43
60	0.24	0.25	0.17	0.07	0.49

is likely to be entrained by the organic phase in the form of $MgCl_2$. Therefore, Equation (16) is proposed [41,42], where y and z represent the molecular numbers of P507 (HL) and TBP involved in the reaction, respectively, and their values can be further determined by subsequent model calculation.

TBP and P507 participate in the equilibria of Eq. (5)–(8) as extractants, and there is interaction between them in the organic phase. Barker et al.[43] reported one possible reaction between TBP and P204 (di(2-ethylhexyl) phosphoric acid, D2EHPA), in which one P204 molecule and one TBP molecule combined with each other via hydrogen bond. Atefeh et al.[44] obtained the same results by analyzing the mixture of TBP, P204 and kerosene with infrared spectroscopy. Since the structures and properties of P507 and P204 are similar [45,46], it is inferred that P507 and TBP may have the same interaction (Eq. (9)). In addition, studies have shown that one P204 molecule will bind to one or two TOPO (trioctylphosphane oxide) molecules through hydrogen bond [47-49]. Since both TBP and TOPO are neutral organic phosphate extractants with similar structures and properties, it is inferred that TBP and P507 also have the same interaction (Eq. (10)). The equilibria that may occur when Fe^{3+} forms different ferric chloride complexes in chloride solution were shown in Eq. (1)–(4). Eq. (17) is proved to occur only in stripping and not in extraction in the following model calculations with details shown in Section 4.2.

2.2. Material balance relationships

According to the reaction equilibrium equations and corresponding equilibrium constants expressed in Table 1, the material balance equations of Fe^{3+}, Mg^{2+}, Li^{+}, H^{+}, P507(HL), TBP and Cl- are listed and simplified as follows.

$$[\mathrm{Fe}]_0 = [\mathrm{Fe}^{3+}] \times \left(\alpha + R \times \left[\overline{\mathrm{TBP}}\right][\mathrm{Cl}^-]^4 \left(k_5 k_4 \left[\overline{\mathrm{TBP}}\right][\mathrm{H}^+] + k_4[\mathrm{Li}^+]\left(k_{L,1} + k_{L,2}\left[\overline{\mathrm{TBP}}\right]\right) + 2k_4 k_{M,1}\left[\mathrm{Mg}^{2+}\right] + k_2 k_{Fe} k_{HL,2}\frac{\left[\overline{\mathrm{TBP}}\right]\left[\overline{\mathrm{HL}}\right]^2}{[\mathrm{H}^+][\mathrm{Cl}^-]^2} \right) \right) \tag{18}$$

$$[\mathrm{Mg}]_0 = \left[\mathrm{Mg}^{2+}\right]\left(1 + R \times \left(k_4^2 k_{M,1}\left[\overline{\mathrm{TBP}}\right]^x\left[\mathrm{Fe}^{3+}\right]^2[\mathrm{Cl}^-]^8 + k_{M,2}\left[\overline{\mathrm{HL}}\right]^y\left[\overline{\mathrm{TBP}}\right]^z[\mathrm{Cl}^-]^2\right)\right) \tag{19}$$

$$[\mathrm{Li}]_0 = [\mathrm{Li}^+] \times \left(1 + R \times k_4\left[\mathrm{Fe}^{3+}\right][\mathrm{Cl}^-]^4\left[\overline{\mathrm{TBP}}\right]\left(k_{L,1} + k_{L,2}\left[\overline{\mathrm{TBP}}\right]\right)\right) \tag{20}$$

$$[\mathrm{H}^+]_0 + R\left[\overline{\mathrm{HL}}\right]_0 = \left[\overline{\mathrm{HL}}\right](k_{HL,1} + R) + [\mathrm{H}^+] + R \times \left(2k_{HL,2}\left[\overline{\mathrm{HL}}\right]^2\left(1 + k_{T,2}\left[\overline{\mathrm{TBP}}\right] + k_{T,3}\left[\overline{\mathrm{TBP}}\right]^2\right) + yk_{M,2}\left[\overline{\mathrm{HL}}\right]^y\left[\overline{\mathrm{TBP}}\right]^z\left[\mathrm{Mg}^{2+}\right][\mathrm{Cl}^-]^2 + \left[\overline{\mathrm{TBP}}\right]^2\left[\mathrm{Fe}^{3+}\right][\mathrm{Cl}^-]^4\left(k_4k_5[\mathrm{H}^+] + k_2 k_{Fe} k_{HL,2}\frac{\left[\overline{\mathrm{HL}}\right]^2}{[\mathrm{Cl}^-]^2[\mathrm{H}^+]}\right) + k_{T,4}\left[\overline{\mathrm{TBP}}\right][\mathrm{Cl}^-] \right) \tag{21}$$

$$[\mathrm{Cl}]_0 = \left([\mathrm{Cl}^-]\beta + [\mathrm{Cl}^-]^2 R \times \left(\left[\mathrm{Fe}^{3+}\right][\mathrm{Cl}^-]^2\left(4k_4k_5\left[\overline{\mathrm{TBP}}\right]^2[\mathrm{H}^+] + k_4\left[\overline{\mathrm{TBP}}\right][\mathrm{Li}^+]\left(4k_{L,1} + 4k_{L,2}\left[\overline{\mathrm{TBP}}\right]\right)\right) + \left[\mathrm{Mg}^{2+}\right]\left(8k_4^2k_{M,1}\left[\overline{\mathrm{TBP}}\right]^x\left[\mathrm{Fe}^{3+}\right]^2[\mathrm{Cl}^-]^6 + 2k_{M,2}\left[\overline{\mathrm{HL}}\right]^y\left[\overline{\mathrm{TBP}}\right]^z\right) + k_{T,4}\frac{\left[\overline{\mathrm{TBP}}\right][\mathrm{H}^+]}{[\mathrm{Cl}^-]} + 2k_2k_{Fe}k_{HL,2}\frac{\left[\overline{\mathrm{TBP}}\right]^2\left[\overline{\mathrm{HL}}\right]^2\left[\mathrm{Fe}^{3+}\right]}{[\mathrm{H}^+]} \right) \right) \tag{22}$$

$$R\left[\overline{\mathrm{HL}}\right]_0 = \left[\overline{\mathrm{HL}}\right] \times \left(\begin{array}{c} k_{HL,1}\left(1 + k_{HL,3}\frac{1}{[\mathrm{H}^+]}\right) \\ +R \times \left(2k_{HL,2}\left[\overline{\mathrm{HL}}\right]\left(1 + k_{T,2}\left[\overline{\mathrm{TBP}}\right] + k_{T,3}\left[\overline{\mathrm{TBP}}\right]^2 + k_2k_{Fe}\frac{\left[\overline{\mathrm{TBP}}\right]^2[\mathrm{Fe}^{3+}][\mathrm{Cl}^-]^2}{[\mathrm{H}^+]}\right) + yk_{M,2}\left[\overline{\mathrm{HL}}\right]^{y-1}\left[\overline{\mathrm{TBP}}\right]^z[\mathrm{Mg}^{2+}][\mathrm{Cl}^-]^2 + 1 \right) \end{array} \right) \tag{23}$$

$$\left[\overline{\mathrm{TBP}}\right]_0 = \left[\overline{\mathrm{TBP}}\right] \times \left(\begin{array}{l} \frac{k_{T,1}}{R} + k_{HL,2}\left[\overline{\mathrm{HL}}\right]^2\left(k_{T,2} + 2k_{T,3}\left[\overline{\mathrm{TBP}}\right] + 2k_2k_{Fe}\frac{\left[\overline{\mathrm{TBP}}\right][\mathrm{Fe}^{3+}][\mathrm{Cl}^-]^2}{[\mathrm{H}^+]}\right) \\ + k_4[\mathrm{Fe}^{3+}][\mathrm{Cl}^-]^4\left(2k_5\left[\overline{\mathrm{TBP}}\right][\mathrm{H}^+] + k_{L,1}[\mathrm{Li}^+] + 2k_{L,2}\left[\overline{\mathrm{TBP}}\right][\mathrm{Li}^+]\right) + xk_4^2k_{M,1}\left[\overline{\mathrm{TBP}}\right]^{x-1}[\mathrm{Fe}^{3+}]^2[\mathrm{Cl}^-]^8[\mathrm{Mg}^{2+}] + 1 \\ + zk_{M,2}\left[\overline{\mathrm{HL}}\right]^y\left[\overline{\mathrm{TBP}}\right]^{z-1}[\mathrm{Mg}^{2+}][\mathrm{Cl}^-]^2 + k_{T,4}[\mathrm{H}^+][\mathrm{Cl}^-] \end{array} \right) \tag{24}$$

where $[\mathrm{Fe}^{3+}]_0$, $[\mathrm{Mg}^{2+}]_0$, $[\mathrm{Li}^+]_0$, $[\mathrm{H}^+]_0$, $[\mathrm{Cl}^-]_0$, $\left[\overline{\mathrm{HL}}\right]_0$ and $\left[\overline{\mathrm{TBP}}\right]_0$ represent the initial concentrations of Fe^{3+}, Mg^{2+}, Li^+, H^+, Cl^-, HL and TBP. $[\mathrm{Fe}^{3+}]$, $[\mathrm{Mg}^{2+}]$, $[\mathrm{Li}^+]$, $[\mathrm{H}^+]$ and $[\mathrm{Cl}^-]$ represent the equilibrium concentrations of Fe^{3+}, Mg^{2+}, Li^+, H^+ and Cl^- in the aqueous phase. $\left[\overline{\mathrm{HL}}\right]$ and $\left[\overline{\mathrm{TBP}}\right]$ represent the equilibrium concentrations of HL and TBP in the organic phase. R represents the phase ratio (O/A). In Eqs. (18) and (22), α and β are expressed as follows ($i = 1 \sim 4$).

$$\alpha = \left(1 + \sum_i^4 k_i[\mathrm{Cl}^-]^i\right) \tag{25}$$

$$\beta = \left(1 + \sum_i^4 i \cdot k_i[\mathrm{Fe}^{3+}][\mathrm{Cl}^-]^{i-1}\right) \tag{26}$$

2.3. Model solving

Among the above seven equations (Eq. (18)–(24)), the seven unknowns are $[\mathrm{Fe}^{3+}]$, $[\mathrm{Mg}^{2+}]$, $[\mathrm{Li}^+]$, $[\mathrm{H}^+]$, $[\mathrm{Cl}^-]$, $\left[\overline{\mathrm{HL}}\right]$ and $\left[\overline{\mathrm{TBP}}\right]$. After giving the values of any apparent equilibrium constants k_1, k_2, k_3, k_4, $k_{HL,1}$, $k_{HL,2}$, $k_{HL,3}$, $k_{T,1}$, $k_{T,2}$, $k_{T,3}$, $k_{T,4}$, k_5, $k_{L,1}$, $k_{L,2}$, $k_{M,1}$, $k_{M,2}$, k_{Fe}, the seven equations can be solved. Once the equilibrium concentration of each ion in the aqueous phase ($[\mathrm{Fe}^{3+}]$, $[\mathrm{Mg}^{2+}]$, $[\mathrm{Li}^+]$) is obtained, the extraction efficiency (%E) and stripping efficiency (%S) of each ion can be calculated according to Eq. (27) and Eq. (28). By minimizing the objective function F (Eq. (29)), the empirical values of the apparent equilibrium constants (*k*-values) can be optimized. Fig. 1 showed the flowchart of the optimum equilibrium constants determination by the least-squares method.

$$\%E = \frac{C_0 \cdot V_0 - C_{\mathrm{aq}} \cdot V_{\mathrm{aq}}}{C_0 \cdot V_0} \times 100\% \tag{27}$$

$$\%S = \left(1 - \frac{C_{aq,s}V_{\mathrm{aq},s}}{C_0V_0 - C_{aq}V_{aq}}\right) \times 100\backslash\% \tag{28}$$

where C_0 and V_0 are the initial element concentration and the volume of feed solution, respectively. C_{aq} and V_{aq} are the equilibrium element concentration and the volume of aqueous phase, respectively. $C_{\mathrm{aq,s}}$ and $V_{\mathrm{aq,s}}$ are the equilibrium element concentration in the stripping aqueous phase and the volume of the stripping aqueous phase, respectively.

$$F = \sum_{i=1}^n \left[\frac{E^{cal.} - E^{exp.}}{E^{exp.}}\right]^2 or F = \sum_{i=1}^n \left[\frac{S^{cal.} - S^{exp.}}{S^{exp.}}\right]^2 \tag{29}$$

The concentrations of $[\mathrm{Fe}^{3+}]$, $[\mathrm{Mg}^{2+}]$, $[\mathrm{Li}^+]$, $[\mathrm{H}^+]$, $[\mathrm{Cl}^-]$, $\left[\overline{\mathrm{HL}}\right]$ and $\left[\overline{\mathrm{TBP}}\right]$ in the nonlinear equations (Eq. (18)–(24)) are solved by means of the fsolve function in the computer numerical analysis commercial software MATLAB. The apparent equilibrium constants k_1 to k_4 and $k_{\mathrm{T},4}$ were taken from the literature [39,50-52], and k_5 was adopted from our previous work [15]. The parameters $k_{\mathrm{HL},1}$, $k_{\mathrm{HL},2}$, $k_{\mathrm{HL},3}$, $k_{\mathrm{T},1}$, $k_{\mathrm{T},2}$, $k_{\mathrm{T},3}$, $k_{\mathrm{L},1}$, $k_{\mathrm{L},2}$, $k_{\mathrm{M},1}$, $k_{\mathrm{M},2}$, k_{Fe} and x, y, z are determined by minimizing the values of Eq. (29) using lsqcurvefit MATLAB function.

3. Experimental

The experimental data of this paper were from our previous study

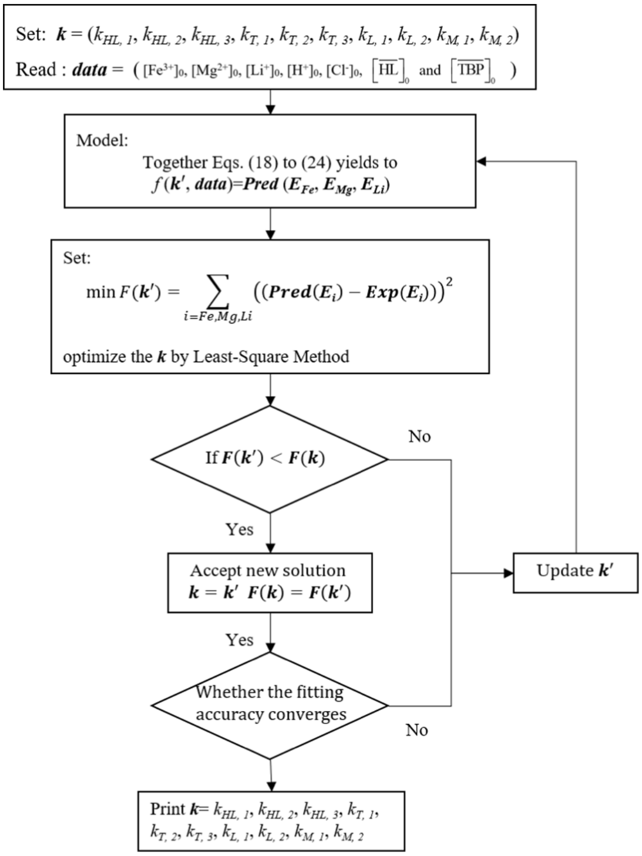

Fig. 1. Flowchart of the optimum equilibrium constants determination by the least-squares method.

[33], the reagents used and solvent extraction procedure are as follows.

3.1. Reagents

$MgCl_2$ (>99%), $FeCl_3$ (>98%) and HCl (37 wt%) were purchased from Beijing Chemical Works. TBP (>98.5%) and P507 (>95%) were provided by Shanghai Rare Earth Chemical Co., Ltd. Sulfonated kerosene (MW = 142–254) was purchased from Sinopharm Group Chemical Reagent Co. Organic phases were prepared by mixing TBP and P507 with kerosene according to the required volume ratio. The treated East Tajinar Salt Lake brine was obtained from Qinghai Salt Lake BYD Resources Development Co., Ltd. and subjected to acidification - crystallization for B removal before lithium extraction. The composition of the brine is shown in Table 3.

3.2. Solvent extraction procedure

Organic phases containing required volume ratio of TBP and P507 pre-loaded with approximately 14 $g{\cdot}L^{-1}$ Fe^{3+} in kerosene were placed in contact with the treated East Tajinar Salt Lake brine after B removed in 150 mL hexagonal jars to extract lithium, shaken in a mechanical shaker (HD-100B, Jintan Yineng, China) with designated O/A ratios (80 mL/mL) at 20 ± 2 °C for 20 min, and then allowed to settle for 30 min to separate the phases. Scrubbing and stripping experiments were carried out using the same method. Aqueous samples were taken from the bottom phases using a syringe with a tube extender for the determination of metal concentrations. The concentrations of Li^+, Mg^{2+} and B in the organic phases were determined after stripping with 6 $mol{\cdot}L^{-1}$ HCl, and Fe^{3+} in the organic phases was calculated by mass balance based on its aqueous concentration. The concentrations in the aqueous samples were determined by inductively coupled plasma-optical emission spectroscopy (ICP-OES, Optima 5300 V, Pekin-Elmer, USA) after dilution to a proper concentration range.

Table 3
Composition of the treated East Tajinar Salt Lake brine after the removal of B.

Component	Li^+	Mg^{2+}	B	Na^+	K^+	pH
Concentration/($g{\cdot}L^{-1}$)	5.02	108.10	2.23	1.31	0.59	0.86

4. Results and discussion

4.1. Thermodynamic modelling of extraction

The extraction of Li^+ and Mg^{2+} from the old brine of East Taijinar Salt Lake after B removal by TBP/P507/$FeCl_3$ system under different conditions were modelled with the results shown in Fig. 2 (The experimental data were from Figs. 2–5 of previous study [33]). The experimental and calculated values of Li^+ and Mg^{2+} extraction efficiency under different conditions fitted well, and Fig. 3 showed that their percentage error was about 20%. The average relative absolute deviation AARD of the experimental and calculated values of Li^+ extraction efficiency under different conditions was less than 10%. The definition of percentage error (PE%) and AARD was expressed in Eq. (30) and Eq. (31), respectively. Generally, the percentage error and AARD within 20% indicate that the model fits well [36,53-56].

The empirical values of the apparent equilibrium constants (k-value) in Table 4 were optimized by fitting the calculated values to the experimental data. The k-values of Li^+ and H^+ extraction were the maxima, indicating that their extraction ability was the optimal in the TBP/P507/$FeCl_3$ system. The k-values of Li^+ coordinated with one TBP molecule and two TBP molecules (Eq. (13) and (14)) were $k_{L,1} = 140$ and $k_{L,2} = 200.56$, respectively. It showed that Li^+ tended to coordinate with two TBP molecules in the extraction, which was consistent with the extracted species $[Li(TBP)_2][FeCl_4]$ established in our previous study [15]. However, the k-value of Li extraction (Eq. (14)) calculated from the experimental data in the previous study was 120.6, which was different from the modelled $k_{L,2} = 200.56$. Considering that the k-value of the modelling was the result of comprehensively fitting the extraction of Li^+ and Mg^{2+} under different conditions and the stripping of different ions (section 4.2), the $k_{L,2}$ value of 200.56 obtained by the modelling was further modified. The k-value of the reaction of H^+ extraction forming $[H(TBP)_2][FeCl_4]$ (Eq. (12)) was $k_5 = 799.87$, whereas the equilibrium constant for H^+ extraction forming $HCl{\cdot}TBP$ (Eq. (11)) was $k_{T,4} = 0.03$, much lower than k_5, indicating that H^+ tended to form $[H(TBP)_2][FeCl_4]$ in the presence of Fe^{3+}[50,57].

According to the model calculation, the extraction of Mg^{2+} was mainly via coordination with six TBP molecules and then combination with $FeCl_4^-$ for charge balance (Eq. (15)). It was reported that Mg^{2+} could exist stably in the form of $[Mg(H_2O)_6]^{2+}$ in aqueous solution [58,59], thus it was speculated that Mg^{2+} also tended to form a stable six coordination structure with TBP molecules after entering the organic phase. Meanwhile, Mg^{2+} was also extracted by TBP and P507 in the form of $MgCl_2$ (Eq. (16)). However, the k-value of this reaction $k_{M,2} = 3.7 \times 10^{-4}$ was much lower than $k_{M,1} = 10$ of Eq. (15). The corresponding k-value of Eq. (5) and (8) involved in TBP and P507 were very small, indicating that their loss in the aqueous phase was negligible. The k-value of the interaction equilibrium (Eq. (9) and (10)) of TBP and P507 was also low, showing that their actual concentration in the organic phase was basically not affected by their mutual interaction.

$$PE\backslash\% = \left|\frac{E^{cal.} - E^{exp.}}{E^{exp.}}\right| \times 100\backslash\% \text{ or} PE\backslash\% = \left|\frac{S^{cal.} - S^{exp.}}{S^{exp.}}\right| \times 100\% \tag{30}$$

$$AARD = \frac{1}{n}\sum_{i=1}^{n}\left|\frac{E^{cal.} - E^{exp.}}{E^{exp.}}\right| \text{or} AARD = \frac{1}{n}\sum_{i=1}^{n}\left|\frac{S^{cal.} - S^{exp.}}{S^{exp.}}\right| \tag{31}$$

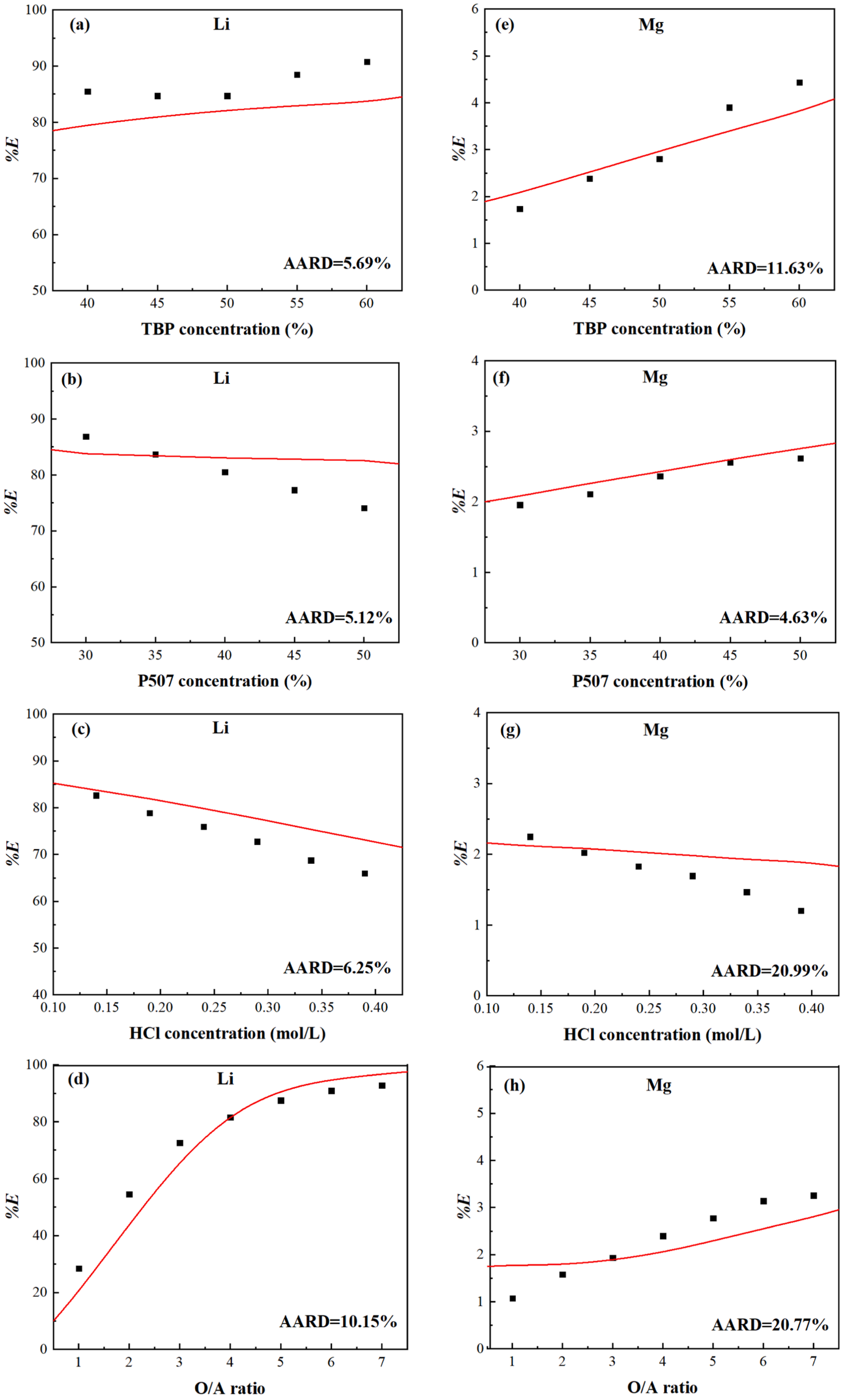

Fig. 2. Fitting results of experimental values (points) and calculated values (lines) of extraction efficiency of Li^+ and Mg^{2+} under different conditions (Constant initial concentration. $[Li^+]_0$ = 0.72 mol L^{-1}, $[Mg^{2+}]_0$ = 4.96 mol L^{-1}, $[Fe^{3+}]_0$ = 0.96 mol L^{-1}. **(a)(e)** $[P507]_0$ = 0.92 mol L^{-1}, $[H^+]_0$ = 0.14 mol L^{-1}, O/A = 4; **(b)(f)** $[TBP]_0$ = 1.47 mol L^{-1}, $[H^+]_0$ = 0.14 mol/L, O/A = 4; **(c)(g)** $[TBP]_0$ = 1.47 mol L^{-1}, $[P507]_0$ = 0.92 mol L^{-1}, O/A = 4; **(d)(h)** $[TBP]_0$ = 1.47 mol L^{-1}, $[P507]_0$ = 0.92 mol L^{-1}, $[H^+]_0$ = 0.14 mol L^{-1}.)

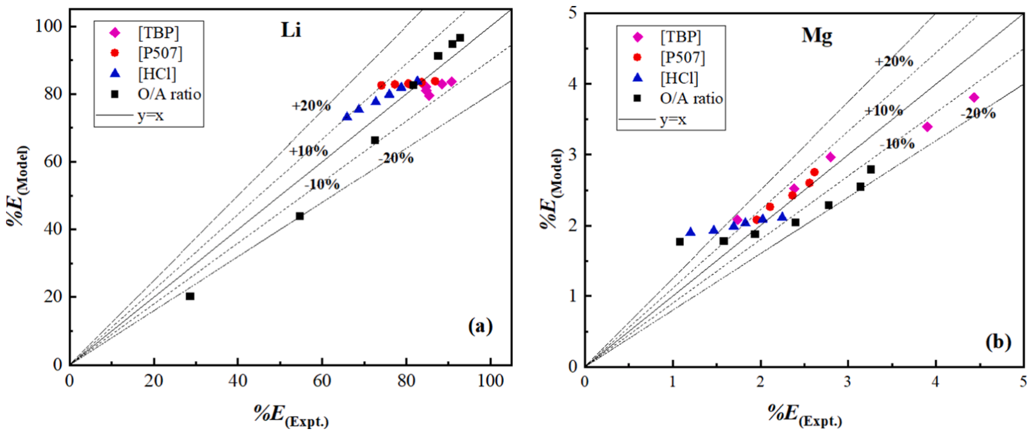

Fig. 3. Comparison of experimental and calculated values (a) extraction efficiency of Li^+; (b) extraction efficiency of Mg^{2+}.

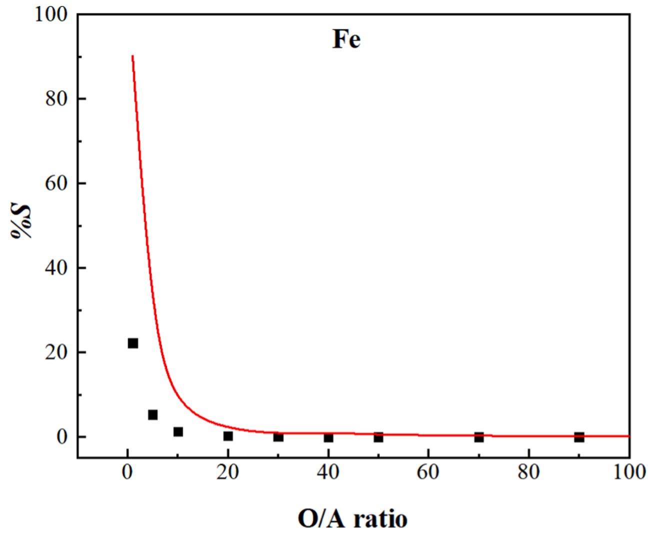

Fig. 4. Fitting results of experimental values (points) and calculated values (lines) of stripping efficiency of Fe^{3+} under different O/A ratios (Without Eq. (17). Constant initial concentrations. $[TBP]_0 = 1.47$ mol L^{-1}, $[P507]_0 = 0.92$ mol L^{-1}.)

4.2. Thermodynamic modelling of stripping

The reactions listed in Table 4 are involved in Li^+ extraction with the TBP/P507/$FeCl_3$ system (mainly forward reaction), these reactions will also occur in Li^+ stripping (mainly reverse reaction). Therefore, these reactions were used to model the stripping of Li^+, Mg^{2+} and Fe^{3+} from the old brine of East Taijinar Salt Lake after B removal under different O/A ratios (The experimental values were from Fig. 9 of our previous study [33]). However, the calculated and experimental values of each ion were poorly fitted, especially the stripping of Fe^{3+} shown in Fig. 4. When O/A ratio was 1, the calculated value of Fe^{3+} stripping was as high as 90.13%, while the actual stripped Fe^{3+} was only 22.21%.

From our previous study on the extraction mechanism with TBP/P507/$FeCl_3$ system [32], it is known that when Li^+ is stripped with water, the structure of $[Li(TBP)_n][FeCl_4]$ is destroyed, Li^+ enters the water phase, and Fe^{3+} is extracted synergistically by TBP and P507 to form $[FeCl_2L\cdot(HL)\cdot 2TBP]$ as shown in Eq. (17), making Fe^{3+} stably maintained in the organic phase. Since Eq. (17) is not taken into account in the result of Fig. 4, it is only considered that the structure of $[Li(TBP)_n][FeCl_4]$ is destroyed during water stripping, and both Li^+ and Fe^{3+} enter the aqueous phase, resulting in abnormally high stripping efficiency of Fe^{3+} at low O/A ratio. However, when Eq. (17) is taken into account in the reactions listed in Table 4 and applied to the model, the calculated values of each ion stripping fitted well with the experimental values, as shown in Fig. 5 and Fig. 6. The calculated value of Fe^{3+} stripping efficiency decreased at the low O/A ratio, and the optimized *k*-value of Eq. (17) is $k_{Fe} = 150$.

$$FeCl_2^+ + \overline{(HL)_2} + 2\overline{TBP} \rightleftharpoons \overline{FeCl_2L\cdot(HL)\cdot 2TBP} + H^+ k_{Fe} = 150 \quad (17)$$

However, when Eq. (17) and the reaction in Table 4 were applied to remodel the extraction process of Li^+, we got poor fitting results. Especially, the calculated values of Li^+ extraction efficiency under different conditions were much lower than the experimental results. This is attributed to the participation of Fe^{3+} in the extraction by TBP and P507 as expressed by Eq. (17) which consumed large amount of Fe^{3+}, and the amount of Fe^{3+} coordinating with Li^+ was dramatically reduced, resulting in a significant declining in the extraction efficiency of Li^+. According to the previous spectral results [32], Fe^{3+} mainly existed in the form of $FeCl_4^-$ in high Cl^- solution and was extracted by TBP after binding with Li^+, and P507 didn't participate in its extraction under such condition. Therefore, Eq. (17) presented only in stripping but not in extraction.

4.3. Distribution of species in loaded organic phase

4.3.1. Distribution of species in loaded organic phase with TBP concentration

According to the extraction thermodynamic model (applicable conditions: $[Mg^{2+}] > 4$ mol/L, Fe/Li > 1.3 (mole ratio), $[H^+] < 1$ mol/L, [TBP] < 2.5 mol/L, [P507] < 1.5 mol/L, O/A < 10) established in section 4.1, the concentration distribution of each species in the loaded organic phase under different TBP concentrations was calculated and the results were shown in Fig. 7. When the concentration of TBP was 0 ~ 1.1 mol/L, Li^+ mainly bound to one TBP molecule to form $[Li(TBP)][FeCl_4]$. However, with the continuous increase of TBP concentration, the concentration of $[Li(TBP)_2][FeCl_4]$ increased and it exceeded the concentration of $[Li(TBP)][FeCl_4]$ and became the main form of Li^+ in the organic phase. In the experiment, the extraction of Li^+ was the highest at TBP concentration of 1.5 mol/L, Li^+ mainly bound two TBP molecules to form ($[Li(TBP)_2][FeCl_4]$). H^+ was basically combined with Fe^{3+} to form $[H(TBP)_2][FeCl_4]$, and its concentration in the organic phase increased slowly with the increase of TBP concentration. However, its concentration was significantly lower than that of extracted Li^+ species. The concentration of HCl·TBP was very low, far lower than the concentration of $[H(TBP)_2][FeCl_4]$, and gradually dropped with the increase of TBP concentration.

Mg^{2+} was primarily entrained into the organic phase by TBP and P507 in the form of $[MgCl_2]HL\cdot TBP_2$ rather than $[Mg(TBP)_6][FeCl_4]_2$, mainly because most of the Fe^{3+} in the organic phase was used to

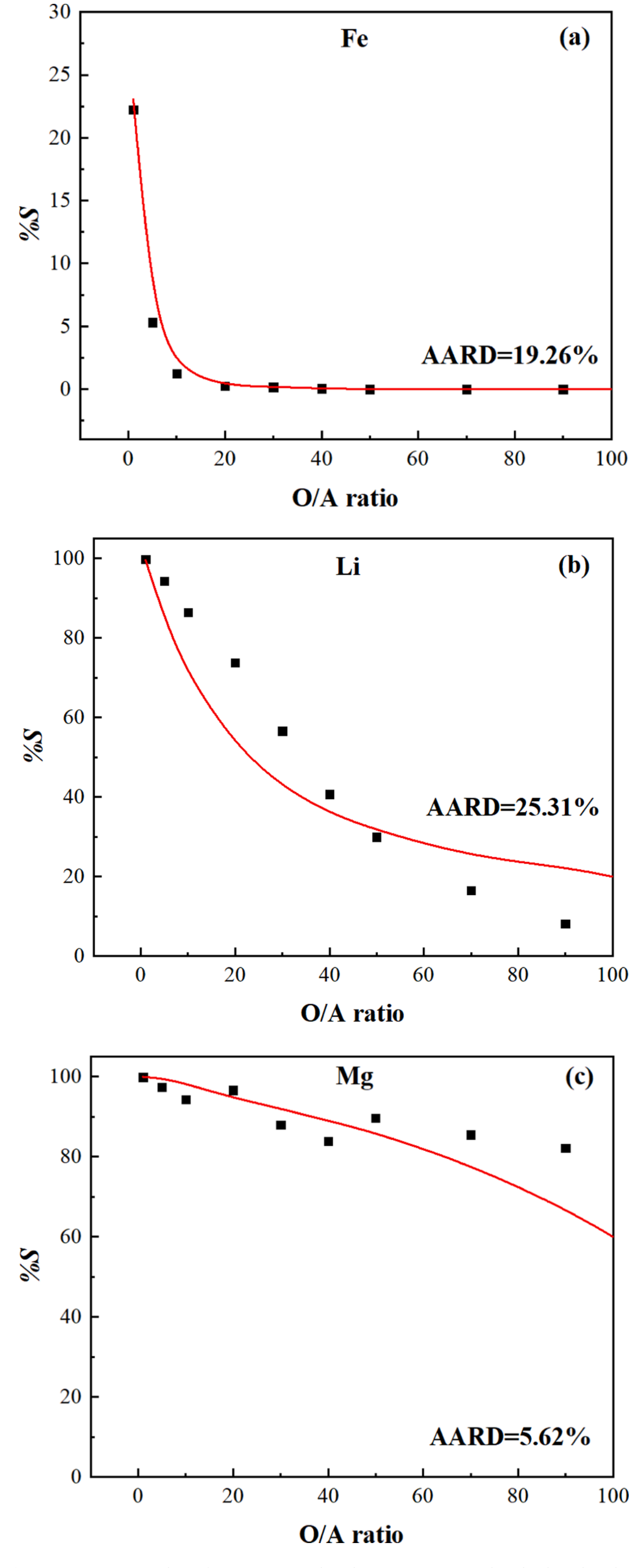

Fig. 5. Fitting results of experimental values (points) and calculated values (lines) of stripping efficiency of Fe^{3+}, Li^{+} and Mg^{2+} under different O/A ratios (Including Eq. (17). Constant initial concentrations. $[TBP]_0 = 1.47$ mol L^{-1}, $[P507]_0 = 0.92$ mol L^{-1}.)

Table 4
Equilibrium and corresponding empirical value of equilibrium constant in Li extraction process in TBP/P507–$FeCl_3$ system.

No.	Equilibrium	Empirical value of equilibrium constant	Ref.
(1)	$Fe^{3+} + Cl^- \rightleftharpoons FeCl^{2+}$	$k_1 = 20.42$	[50-52]
(2)	$Fe^{3+} + 2Cl^- \rightleftharpoons FeCl_2^+$	$k_2 = 95.50$	
(3)	$Fe^{3+} + 3Cl^- \rightleftharpoons FeCl_3$	$k_3 = 15.49$	
(4)	$Fe^{3+} + 4Cl^- \rightleftharpoons FeCl_4^-$	$k_4 = 0.049$	
(5)	$\overline{HL} \rightleftharpoons HL$	$k_{HL,1} = 1.05 \times 10^{-3(*)}$	
(6)	$2\overline{HL} \rightleftharpoons \overline{(HL)_2}$	$k_{HL,2} = 4.35 \times 10^{-2(*)}$	
(7)	$HL \rightleftharpoons L^- + H^+$	$k_{HL,3} = 0.011^{(*)}$	
(8)	$\overline{TBP} \rightleftharpoons TBP$	$k_{T,1} = 4.10 \times 10^{-4(*)}$	
(9)	$\overline{(HL)_2} + \overline{TBP} \rightleftharpoons \overline{(HL)_2 - TBP}$	$k_{T,2} = 0.025^{(*)}$	
(10)	$\overline{(HL)_2} + 2\overline{TBP} \rightleftharpoons \overline{(HL)_2 - (TBP)_2}$	$k_{T,3} = 0.013^{(*)}$	
(11)	$H^+ + Cl^- + \overline{TBP} \rightleftharpoons \overline{HCl \cdot TBP}$	$k_{T,4} = 0.031$	[39]
(12)	$H^+ + FeCl_4^- + 2\overline{TBP} \rightleftharpoons \overline{[H(TBP)_2][FeCl_4]}$	$k_5 = 799.87$	[15]
(13)	$Li^+ + FeCl_4^- + \overline{TBP} \rightleftharpoons \overline{[Li(TBP)][FeCl_4]}$	$k_{L,1} = 140^{(*)}$	
(14)	$Li^+ + FeCl_4^- + 2\overline{TBP} \rightleftharpoons \overline{[Li(TBP)_2][FeCl_4]}$	$k_{L,2} = 200.56^{(*)}$	
(15)	$Mg^{2+} + 2FeCl_4^- + 6\overline{TBP} \rightleftharpoons \overline{[Mg(TBP)_6][FeCl_4]_2}$	$k_{M,1} = 10^{(*)}$	
(16)	$Mg^{2+} + 2Cl^- + \overline{HL} + 2\overline{TBP} \rightleftharpoons \overline{[MgCl_2]HL \cdot TBP_2}$	$k_{M,2} = 3.7 \times 10^{-4(*)}$	

The values of k_1-k_4, $k_{T,4}$, and k_5 were taken from the literature. $^{(*)}$Values deduced by minimization between experimental and calculated values of the extraction and stripping efficiency of the corresponding ions.

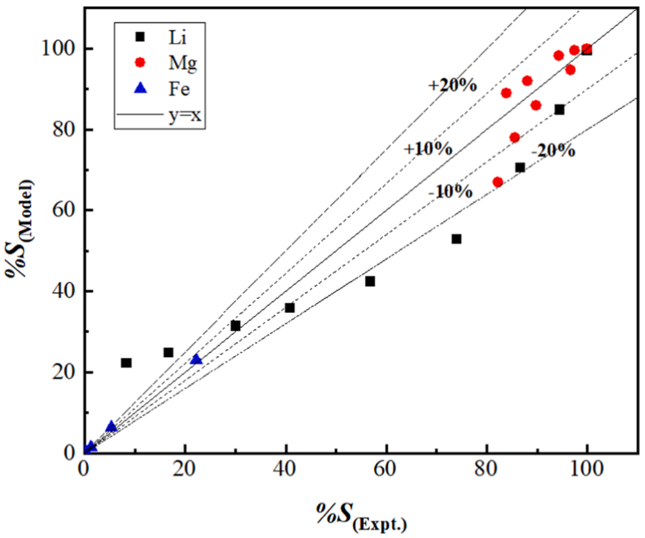

Fig. 6. Comparison of experimental and calculated values of stripping efficiency.

combine with Li^+ and H^+, while the content of the remaining Fe^{3+} combining with Mg^{2+} was very low. The concentration of $[MgCl_2]HL \cdot TBP_2$ increased rapidly with the increase of TBP concentration. When TBP concentration was higher than 1.9 mol/L, this species' concentration exceeded $[Li(TBP)_2][FeCl_4]$. Since the concentration of Mg^{2+} in brine was close to saturation, with the increase of TBP concentration, although its extraction efficiency increased at a low level (Fig. 2 (e)), its loading in the organic phase increased significantly and soon exceeded the loading of Li^+ in the organic phase according to our previous experimental results (Table 3 in [33]). However, Mg^{2+} entrained in the

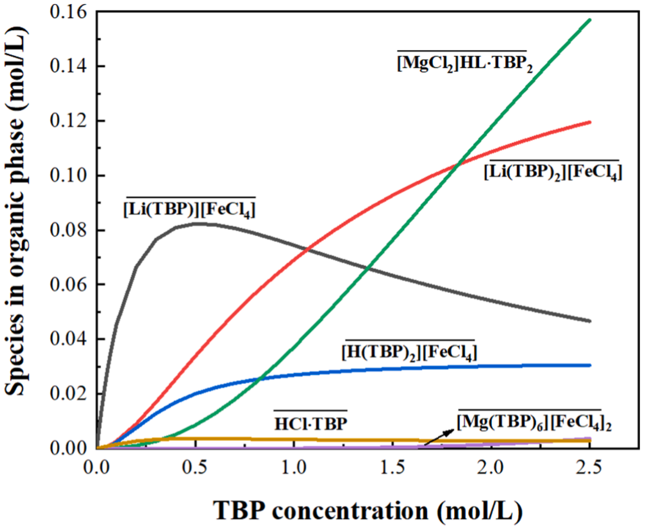

Fig. 7. Species distribution in the loaded organic phase with TBP concentration calculated by the extraction model (Initial concentrations. $[P507]_0 = 0.92$ mol L^{-1}; $[Li^+]_0 = 0.77$ mol L^{-1}, $[Mg^{2+}]_0 = 4.23$ mol L^{-1}, $[Fe^{3+}]_0 = 0.96$ mol L^{-1}, $[H^+]_0 = 0.14$ mol L^{-1}. O/A = 4).

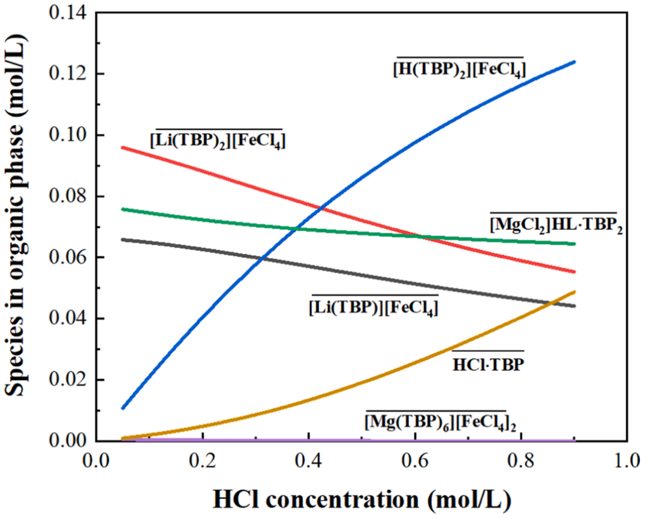

Fig. 8. Species distribution in the loaded organic phase with HCl concentration calculated by the extraction model (The initial concentrations. $[TBP]_0 = 1.47$ mol L^{-1}, $[P507]_0 = 0.92$ mol L^{-1}, $[Li^+]_0 = 0.77$ mol L^{-1}, $[Mg^{2+}]_0 = 4.23$ mol L^{-1}, $[Fe^{3+}]_0 = 0.96$ mol L^{-1}. O/A = 4).

organic phase can be removed by multistage scrubbing with water [33].

4.3.2. Distribution of species in loaded organic phase with HCl concentration

The concentration distribution of each species in the loaded organic phase under different HCl concentrations was calculated by the extraction thermodynamic model and the results are shown in Fig. 8. With the increase of HCl concentration, the concentrations of $[Li(TBP)_2][FeCl_4]$ and $[Li(TBP)][FeCl_4]$ decreased rapidly, while the concentrations of $[H(TBP)_2][FeCl_4]$ and HCl·TBP increased rapidly. When the concentration of HCl was>0.4 mol/L, the concentration of $[H(TBP)_2][FeCl_4]$ exceeded the concentration of extracted Li^+ species. This was mainly because H^+ is extracted more easily than Li^+ ($k_5 = 7998.87 > k_{L,2} = 200.56 > k_{L,1} = 140$), and the extraction of H^+ causes fierce competition against Li^+. Since the concentration of HCl in the feed solution was generally close to 0.14 mol/L, the Li^+ species $[Li(TBP)_2][FeCl_4]$ was still the main component in the organic phase. The concentration of extracted Mg^{2+} species $[MgCl_2]HL\cdot TBP_2$ also decreased with the increase of HCl concentration, but the downward trend was not obvious, indicating that H^+ had little effect on Mg^{2+} extraction.

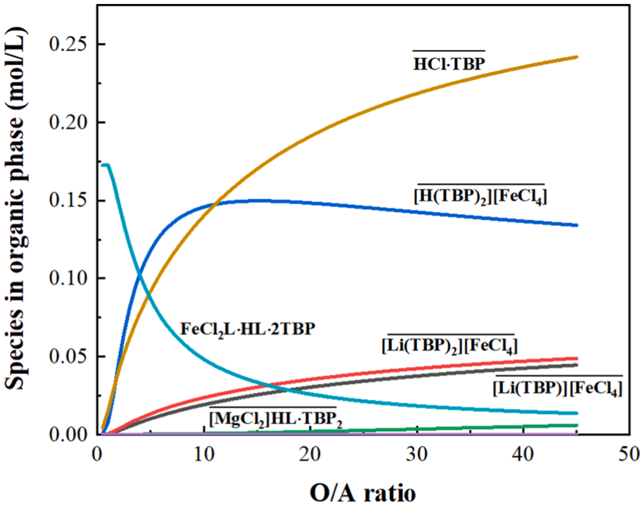

Fig. 9. Species distribution in the organic phase after stripping with O/A ratio calculated by the stripping model (Initial concentrations. $[TBP]_0 = 1.47$ mol L^{-1}, $[P507]_0 = 0.92$ mol L^{-1}).

4.4. Distribution of species in organic phase after stripping

According to the stripping thermodynamic model (applicable conditions: O/A < 100) established in section 4.2, the concentration distribution of each species in the organic phase after stripping under different O/A ratios was calculated and the results are shown in Fig. 9. In the TBP/P507/$FeCl_3$ system, when water was mixed with the loaded organic phase, Li^+ and Mg^{2+} were stripped into the aqueous phase, and Fe^{3+} stably maintained in the organic phase. Therefore, the form distribution of Fe^{3+} in the organic phase has become the focus of attention. It could be seen from Fig. 9 that when the O/A ratio was lower than 5, Fe^{3+} was mainly extracted by TBP and P507 in the form of $FeCl_2L\cdot HL\cdot 2TBP$. However, in TBP/$FeCl_3$ system, when water and loaded organic phase were mixed at the O/A ratio of 1:1, almost 100% of Fe^{3+} was stripped to the aqueous phase, while the stripping of Fe^{3+} was lower than 20% under the same condition in TBP/P507/$FeCl_3$ system [32]. This indicates that P507 played an important role in the high stability of Fe^{3+} species in the organic phase. However, with the continuous increase of O/A ratio, the concentration of $FeCl_2L\cdot HL\cdot 2TBP$ decreased, while the concentration of $[H(TBP)_2][FeCl_4]$ increased and became the main form of Fe^{3+} in the organic phase. This was mainly because with the increase of O/A ratio, the increasing concentration of Cl^- in the aqueous phase facilitated the existence of Fe^{3+} in the form of $FeCl_4^-$, and it combined with H^+ to form $[H(TBP)_2][FeCl_4]$ in the organic phase. High concentration of Cl^- could also promote the extraction of Li^+ and Mg^{2+}, so their extraction species concentration also increased with the increase of O/A ratio. Since a large amount of Mg^{2+} was removed in scrubbing, there was very little Mg^{2+} in the organic phase after stripping. The increase of O/A ratio also led to the accumulation of H^+ in the organic phase, so H^+ existed in the organic phase in the form of HCl·TBP and $[H(TBP)_2][FeCl_4]$.

5. Conclusions

A thermodynamic empirical model has been derived for simulating Li extraction from Mg-rich salt-lake brines with a TBP/P507/$FeCl_3$ system. A good agreement between experimental and calculated extraction and stripping of Li^+, Mg^{2+} and Fe^{3+} under different conditions was obtained by taking into account the $FeCl_2L·HL·2TBP$ formation equilibrium in stripping rather than extraction, and the parameters of *k*-value in each equilibrium were optimized. Using the model to calculate the distribution of species in the organic phase, it was found that Li^+ mainly existed in the organic phase in the form of $[Li(TBP)_2][FeCl_4]$, followed by $[Li(TBP)][FeCl_4]$. When Li^+ was stripped at low O/A ratio, Fe^{3+} was mainly extracted synergistically by TBP and P507 and maintained in the organic phase in the form of $FeCl_2L·HL·2TBP$. However, its concentration decreased with the increase in O/A ratio, and the existing form of Fe^{3+} was mainly transformed into $[H(TBP)_2][FeCl_4]$. The thermodynamic model further elucidates the mechanism of Li^+ extraction from Mg-rich salt-lake brines by TBP/P507/$FeCl_3$ system, and guides the design and development of practical process flow.

CRediT authorship contribution statement

Hui Su: Writing – original draft, Data curation. **Boren Tan:** Investigation. **Jian Zhang:** Formal analysis. **Wensen Liu:** Data curation. **Lina Wang:** Project administration. **Yong Wang:** Writing – review & editing. **Zhaowu Zhu:** Conceptualization, Methodology. **Tao Qi:** Conceptualization.

Declaration of Competing Interest

The authors declare that they have no known competing financial interests or personal relationships that could have appeared to influence the work reported in this paper.

Acknowledgements

This work was supported by the National Natural Science Foundation of China (51774260, 51804289, 21908231), Beijing Municipal Natural Science Foundation (2202053), Key Program of Innovation Academy for Green Manufacture, and Chinese Academy of Sciences (Grand No. IAGM-2019-A15), Key Research Program of Frontier Sciences of Chinese Academy of Sciences (Grant No. QYZDJ-SSW-JSC021).

References

[1] W. Chen, J. Liang, Z. Yang, G. Li, A review of lithium-ion battery for electric vehicle applications and beyond, Energy Procedia 158 (2019) 4363–4368.

[2] C. Zeng, Special research report on lithium industry in 2020, (2020) 7 https://wenku.baidu.com/view/0b358696178884868762caaedd358696178884863383c358696178884868764ba358696178884868764cb358696178884868744d.html.

[3] The World Bank Group, Minerals for Climate Action: The Mineral Intensity of the Clean Energy Transition, (2020) http://pubdocs.worldbank.org/en/961711588875536384/Minerals-for-Climate-Action-The-Mineral-Intensity-of-the-Clean-Energy-Transition.pdf.

[4] JEWELL S, Suzette M, Kimball Mineral Commodity Summaries 2017, Reston: U.S. Geological Survey, 100-101 (2017).

[5] B. Swain, Recovery and recycling of lithium: a review, Sep. Purif. Technol. 172 (2017) 388–403.

[6] P.K. Choubey, M.-S. Kim, R.R. Srivastava, J.-C. Lee, J.-Y. Lee, Advance review on the exploitation of the prominent energy-storage element: Lithium. Part I: From mineral and brine resources, Miner. Eng. 89 (2016) 119–137.

[7] X. Deng, C. Zhu, Y. Shi, J. Fan, F. Fan, B. Qing, Y. Zhang, W. Zhang, J. Yang, Y. Li, The Current Situation of Qinghai Salt Lake Lithium Resources Development and the Suggestions for Lithium Industry, J. Salt Lake Res. 26 (2018) 11–18.

[8] M. Zheng, X. Hou, Comprehensive utilization and sustainable development strategy of Qinghai Salt Lake Resources, Sci. Technol. Rev. 35 (2017) 11–13.

[9] Z. Li, J. Mercken, X. Li, S. Riaño, K. Binnemans, Efficient and sustainable removal of magnesium from brines for lithium/magnesium separation using binary extractants, ACS Sustain, Chem. Eng. 7 (23) (2019) 19225–19234.

[10] Z. Li, K. Binnemans, Mechanism of Ferric Chloride Facilitating Efficient Lithium Extraction from Magnesium-Rich Brine with Tri- n -butyl Phosphate, Ind. Eng. Chem. Res. 60 (23) (2021) 8538–8547.

[11] H.F. Li, L.J. Li, W. Li, Y.Q. Zhou, The Key Factors and Mechanism Study on Lithium Extraction by TBP-$FeCl_3$ extraction system, Chem. Phys. Lett. 754 (2020) 1–7.

[12] Z. Zhou, J. Fan, X. Liu, Y. Hu, X. Wei, Y. Hu, W. Wang, Z. Ren, Recovery of lithium from salt-lake brines using solvent extraction with TBP as extractant and $FeCl_3$ as co-extraction agent, Hydrometallurgy 191 (2020) 1–8.

[13] D. Shi, L. Zhang, X. Peng, L. Li, F. Song, F. Nie, L. Ji, Y. Zhang, Extraction of lithium from salt lake brine containing boron using multistage centrifuge extractors, Desalination 441 (2018) 44–51.

[14] J. Song, H. Tao, H. Qiu, X. Li, H. Tao, Recovery of lithium from salt lake brine of high Mg/Li ratio using $Na[FeCl_4 * 2TBP]$ as extractant: Thermodynamics, kinetics and processes, Hydrometallurgy 173 (2017) 63–70.

[15] H. Su, Z. Li, Z. Zhu, L. Wang, T. Qi, Extraction relationship of Li^+ and H^+ using tributyl phosphate in the presence of Fe(III), Sep. Sci. Technol. 55 (2020) 1677–1685.

[16] C. Zhang, Y. Mu, S. Zhao, W. Zhang, Y. Wang, Lithium extraction from synthetic brine with high Mg^{2+}/Li^+ ratio using the polymer inclusion membrane, Desalination 496 (2020), 114710.

[17] X. Li, Y. Mo, W. Qing, S. Shao, C.Y. Tang, J. Li, Membrane-based technologies for lithium recovery from water lithium resources: A review, Journal of Membrane Science 591 (2019) 117317, https://doi.org/10.1016/j.memsci.2019.117317.

[18] G. Soumaya, C. Alexandre, Recent advances on electrodialysis for the recovery of lithium from primary and secondary resources, Hydrometallurgy 189 (2019).

[19] D. Weng, H.Y. Duan, Y.C. Hou, J. Huo, L. Chen, F. Zhang, J.D. Wang, Introduction of manganese based lithium-ion Sieve-A review, Prog. Natural Sci. Mater. Int. 30 (2020) 139–152.

[20] H. Jiang, Y. Yang, S. Sun, J. Yu, Adsorption of lithium ions on lithium-aluminum hydroxides: Equilibrium and kinetics, Canadian J. Chem. Eng. 98 (2) (2020) 544–555.

[21] P. Xu, J. Hong, X.M. Qian, Z.W. Xu, H. Xia, X.C. Tao, Z.Z. Xu, Q.Q. Ni, Materials for lithium recovery from salt lake brine, J. Mater. Sci. 56 (2021) 16–63.

[22] Z.W. Yuan, Y.X. Yu, L. Wei, C. Wang, X. Zhong, X. Sui, Z.X. Yu, D.S. Han, S.H. Y. Chen, Thermo-osmosis-Coupled Thermally Regenerative Electrochemical Cycle for Efficient Lithium Extraction, ACS Appl. Mater. Inter. 13 (2021) 6276–6285.

[23] S. Kim, H. Joo, T. Moon, S.H. Kim, J. Yoon, Rapid and selective lithium recovery from desalination brine using an electrochemical system, Environ. Sci.-Proc. Imp. 21 (2019) 667–676.

[24] W. Xiang, S. Liang, Z. Zhou, W. Qin, W. Fei, Lithium recovery from salt lake brine by counter-current extraction using tributyl phosphate/$FeCl_3$ in methyl isobutyl ketone, Hydrometallurgy 171 (2017) 27–32.

[25] W. Xiang, S. Liang, Z. Zhou, W. Qin, W. Fei, Extraction of lithium from salt lake brine containing borate anion and high concentration of magnesium, Hydrometallurgy 166 (2016) 9–15.

[26] Z. Zhou, S. Liang, W. Qin, W. Fei, Extraction equilibria of lithium with tributyl phosphate, diisobutyl ketone, acetophenone, methyl isobutyl ketone, and 2-heptanone in kerosene and $FeCl_3$, Ind. Eng. Chem. Res. 52 (2013) 7912–7917.

[27] Z. Zhou, Q. Wei, L. Yang, W. Fei, Extraction equilibria of lithium with tributyl phosphate in kerosene and $FeCl_3$, J. Chem. Eng. Data 57 (2012) 82–86.

[28] C. Shi, Y. Jia, Y. Jing, Lithium and magnesium separation from salt lake brine by ionic liquids containing tributyl phosphate, CIESC J. 66 (2015) 253–259.

[29] V.I. Kuz'min, N.V. Gudkova, Extraction of lithium using TBP and the noncoordinating cation exchanger tetraphenylborate: principles of selectivity from sodium and higher-valent cations, Solvent Extr. Ion Exch. 33 (2) (2015) 183–195.

[30] C. Shi, J. Yan, Y. Jia, Solvent extraction of lithium ions by tri-n-butyl phosphate using a room temperature ionic liquid, J. Mol. Liq. 215 (2016) 640–646.

[31] Yong Wang, Haotian Liu, Jiahui Fan, Xueting Liu, Yafei Hu, Yulei Hu, Zhiyong Zhou, Zhongqi Ren, Recovery of lithium ions from salt lake brine with a high magnesium/lithium ratio using heteropolyacid ionic liquid, ACS Sustain. Chem. Eng. 7 (3) (2019) 3062–3072.

[32] Hui Su, Zheng Li, Jian Zhang, Wensen Liu, Zhaowu Zhu, Lina Wang, Tao Qi, Combining selective extraction and easy stripping of lithium using a ternary synergistic solvent extraction system through regulation of Fe^{3+} coordination, ACS Sustain. Chem. Eng. 8 (4) (2020) 1971–1979.

[33] Hui Su, Zheng Li, Jian Zhang, Zhaowu Zhu, Lina Wang, Tao Qi, Recovery of lithium from salt lake brine using a mixed ternary solvent extraction system consisting of TBP, $FeCl_3$ and P507, Hydrometallurgy 197 (2020) 105487, https://doi.org/10.1016/j.hydromet.2020.105487.

[34] Zhiyong Zhou, Wei Qin, Yifeng Chu, Weiyang Fei, Elucidation of the structures of tributyl phosphate/Li complexes in the presence of $FeCl_3$ via UV–visible, Raman and IR spectroscopy and the method of continuous variation, Chem. Eng. Sci. 101 (2013) 577–585.

[35] Zhiyong Zhou, Wei Qin, Weiyang Fei, Extraction Equilibria of Lithium with Tributyl Phosphate in Three Diluents, J. Chem. Eng. Data 56 (9) (2011) 3518–3522.

[36] K.H. Lum, G.W. Stevens, S.E. Kentish, The modelling of water and hydrochloric acid extraction by tri-n-butyl phosphate, Chem. Eng. Sci. 84 (2012) 21–30.

[37] X.H. Mao, L. Deng, Solvent extraction and separation of hydrochloric acid by TBP from acid leaching solution of titanium-bearing ores, Chem. Res. Appl. 28 (2016) 909–912.

[38] G. Zeming, Z. Shenlin, Extraction of lithium from brine containing high concentration of magnesium by tri-n-butyl phosphate dissolved in kerosene, Chin. J. Chem. Eng. 34–34 (1998).

[39] K. Sarangi, E. Padhan, P. Sarma, K.H. Park, R.P. Das, Removal/recovery of hydrochloric acid using Alamine 336, Aliquat 336, TBP and Cyanex 923, Hydrometallurgy 84 (2006) 125–129.

[40] Y.H. Zhang, L.J. Li, L.J. F., L.M. Ji, Q.R. Xu, G.H. Cehn, Study on mechanism of extraction of lithium from salt lake brine by tributylphosphate, Inorganic Chemicals Industry, 44 (2012) 12-15.

[41] H. Lv, X. Huang, Z. Feng, M. Wang, X. Sun, X. Peng, D. Cui, Y. Hu, Extraction kinetics of neodymium from chloride medium using HEH/EHP saponified with magnesium bicarbonate solution, J. Rare Earths 37 (2019) 305–311.

[42] J.M. Liu, D.S. Tan, J.J. Jiang, B.N. Zhou, Mechanism of extracting magnesium using2-ethylhexyl phosphonic acid mono-2-ethylhexyl ester from sulfate media, Chinese J. Nonferrous Metals 13 (2003) 1574–1577.

[43] H.T. Baker, C.F. Baes, An infra-red and isopiestic investigation of the interaction between di(2-ethylhexyl) phosphoric acid and tri-n-octylphosphine oxide in octane, J. Inorg. Nucl. Chem. 24 (1962) 1277–1286.

[44] A. Azizitorghabeh, F. Rashchi, A. Babakhani, Stoichiometry and structural studies of Fe(III) and Zn(II) solvent extraction using D2EHPA/TBP, Sep. Purif. Technol. 171 (2016) 197–205.

[45] J. Jayachandran, P.M. Dhadke, Liquid-liquid extraction separation of iron (III) with 2-ethyl hexyl phosphonic acid mono 2-ethyl hexyl ester, Talanta 44 (1997) 1285.

[46] J. Zhang, Z.W. Zhu, Z. Lei, L.N. Wang, D.S. Chen, A.F. Yi, H. Su, T. Qi, Preparation of Vanadium Oxalate by Solvent Extraction and Purification with P507 and Its Physicochemical Properties, Chem. J. Chinese Universities 40 (2019) 740–746.

[47] K. Staszak, K. Prochaska, Investigation of the interaction in binary mixed extraction systems by Fourier Transform Infrared Spectroscopy (FT-IR), Hydrometallurgy 90 (2008) 75–84.

[48] H.T. Baker, C.F. BaesJr, An infra-red and isopiestic investigation of the interaction between di(2-ethylhexyl) phosphoric acid and tri-n-octylphosphine oxide in octane, J. Inorg. Nucl. Chem. 24 (1962) 1277–1286.

[49] Beltrami Denis, Cote Gérard, Mokhtari Hamid, Courtaud Bruno, Chagne Alexandre, Modeling of the extraction of uranium (VI) from concentrated phosphoric acid by synergistic mixtures of bis-(2-ethylhexyl)-phosphoric acid and tri-n-octylphosphine oxide, Hydrometallurgy 129–130 (2012) 118–125.

[50] M.S. Lee, G.S. Lee, K.Y. Sohn, Solvent Extraction Equilibria of $FeCl_3$ with TBP, Mater. Trans. 45 (2004) 1859–1863.

[51] L. Manseung, A. Jonggwan, O.H. Youngjoo, Chemical Model of the $FeCl_3$-HCl-H_2O Solutions at 25℃, Mater. Trans. 44 (2003) 957–961.

[52] Y. Belaustegi, M. Olazabal, J. Madariaga, Development of a Modified Bromley's Methodology for the estimation of ionic media effects on solution equilibria Part 4. The chemical model of Fe(III) with the halide ligands in aqueous solution at 25 degrees C, Fluid Phase Equilib. 155 (1999) 21–31.

[53] B. Tan, C. Chang, D. Xu, Y. Wang, T. Qi, Modeling of the Competition between Uranyl Nitrate and Nitric Acid upon Extraction with Tri- n -butyl Phosphate, ACS Omega 5 (2020) 12174–12183.

[54] K.H. Lum, G.W. Stevens, J.M. Perera, S.E. Kentish, The modelling of $ZnCl_2$ extraction and HCl co-extraction by TBP diluted in ShellSol 2046, Hydrometallurgy 133 (2013) 64–74.

[55] Adrien Dartiguelongue, Alexandre Chagnes, Elise Provost, Walter Fürst, Gérard Cote, Modelling of uranium(VI) extraction by D2EHPA/TOPO from phosphoric acid within a wide range of concentrations, Hydrometallurgy 165 (2016) 57–63.

[56] A.E. Giles, C. Aldrich, J.S.J. van, Modelling of rare earth solvent extraction with artificial neural nets, Hydrometallurgy 43 (1-3) (1996) 241–255.

[57] R.K. Mishra, P.C. Rout, K. Sarangi, K.C. Nathsarma, A comparative study on extraction of Fe(III) from chloride leach liquor using TBP, Cyanex 921 and Cyanex 923, Hydrometallurgy 104 (2) (2010) 298–303.

[58] I. Persson, Coordination Chemistry of Metal Ions in Some Oxygen Donor Solvents, Comprehensive Coordination Chem. III (3) (2019) 1–16.

[59] Kenji Waizumi, Hideki Masuda, Nobuhiro Fukushima, A molecular approach to the formation of KCl and $MgCl^+$ ion-pairs in aqueous solution by density functional calculations, Chem. Phys. Lett. 205 (2-3) (1993) 317–323.